Experimental and Numerical Studies on Multicomponent Fuel Spray and Vaporization Processes

J. Senda[1] , D. Kawano[2] , Y. Wada[1] and H. Fujimoto[1]

1. Department of Mechanical Engineering, Doshisha University
Miyakodani 1-3, Tatara, Kyotanabe, 610-0321 JAPAN
2. National Traffic Safety and Environment Laboratory
Jindaiji-higashi-machi 7-42-27, Chofu, Tokyo, 182-0012 JAPAN

Recently, the authors have proposed fuel design approach to control the spray evaporation process and combustion process in internal combustion engines. Here, mixed fuel with high volatility fuel such as gasoline component and low volatility fuel such as diesel gas oil component were used to improve the spray evaporation and to control the ignition property. In the present study, the spray evaporation characteristics of multicomponent fuel (n-pentane and n-tridecane) are examined by use of LIF technique. In addition, the modeling of the spray evaporation is conducted using KIVA3V code to clarify the spatial distribution of each fuel component with the variation of the mixing fraction of each fuel.

1. Introduction

In representative simulation codes for engine spray combustion such as KIVA, FIRE and Star-CD, just a single component fuel could be applied in their original versions. Therefore, the actual mixture properties are never assessed by these simulation codes.
With regard to multicomponent droplet vaporization, Jin and Borman [1] have reported the difference in evaporation rate of each component. Chen et al. [2] have analyzed the evaporation process of a binary fuel considering the species concentration distribution inside the droplet. In connection with the spray dynamics related to the multicomponent fuel, Ayoub and Reitz [3-4] have modeled and calculated the evaporation process for multicomponent droplets and sprays with the consideration of high-pressure effects. They conducted the computations using KIVA-2 code, where the gas-liquid equilibrium was analyzed. Lippert and Reitz [5] proposed a simple evaporation model, where the fuel components were given from the molecular distribution in order to extend the number of fuel species. In the model of Abraham et al. [6], a number of spray droplets were classified into the number of fuel species and each droplet was composed of only one component. On the other hand, Gasoline engine application study was conducted by Nagaoka et al. [7] and they pointed out that 3 components were required at least to estimate the gasoline evaporation process.
We also have reported modeling and measurements on evaporation process of multicomponent fuels focusing on the distillation curve of the multicomponent fuel [8], and the droplet evaporation including the spray-wall interaction process [9].

2. Chemical thermodynamics for multicomponent fuel

Figure 1 shows two-phase region in the pressure-temperature diagram for multicomponent fuels. For the pure substance, the liquid region and the vapor region can be separated accurately by the saturated vapor pressure line. On the other hand, the vapor pressure line of each component pulls each other, and there appears the resultant two-phase region where liquid and vapor phases are mixed. The upper boundary between two-phase region and liquid phase is called as a saturated liquid-line and the lower one between that and the vapor

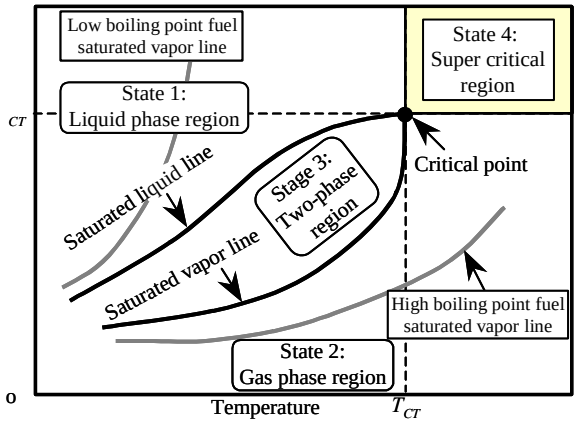

Figure 1 Pressure-temperature diagram for multicomponent fuel

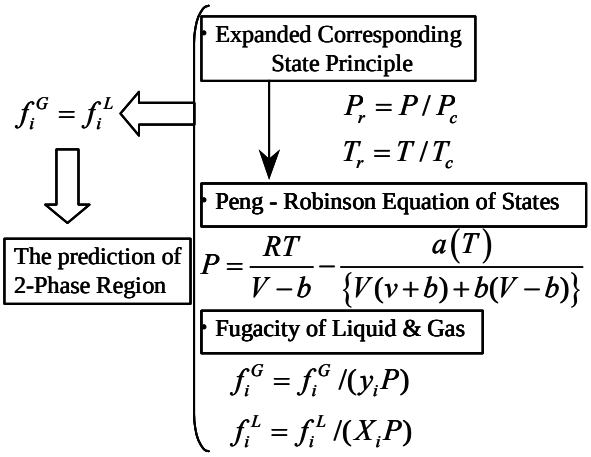

Figure 2 Prediction of two-phase region

phase as a saturated vapor line. Both lines reach the critical point. In the two-phase region, liquid and vapor phases of both components are mixed at a certain molar fraction. And in the case that the liquid pressure exists in the two-phase region, we could get two-phase mixture where the vapor of the lower boiling point component is dominant, and the fuel vaporization is promoted comparing to the pure one of higher boiling point. Thus, the assessment of the two-phase region and vapor-liquid equilibrium analysis is required based on a chemical-thermodynamics approach in order to simulate the evaporation process of multicomponent fuel spray.

For the assessment of the composition of each component inside the two-phase region, the fugacity in vapor-liquid equilibrium theory is introduced. In the assessment, both non-ideal vapor and non-ideal solution are considered to obtain more accurate results. Figure 2 shows a flowchart of the calculation procedure for the two-phase region [8].

3. Experimental procedure

In this study, rapid compression and expansion machine (RCEM) was used for experiments. The chamber shape is a flat disk type with a side injection system. The cylinder wall temperature is adjusted to a predetermined one by supplying hot water into a water jacket. A quartz glass window has been installed in the cylinder head in order to take the spray photography.

For the investigation of the effect of fuel properties on spray characteristics the mixed fuel of n-tridecane (C13, b.p. : 508.7K, mole fraction of n-pentane X_{C5H12}=0.0) and n-pentane (C5, b.p. : 309.3K, X_{C5H12}=1.0) were used. As a mixed fuel, mixed fuels with each mole fraction (C5/C13, X_{C5H12}=0.25, 0.5, 0.75) were used. Table 1 indicates the mixing fraction vol.% of each tracer for LIF. 5.0vol.% acetone (C_3H_6O, b.p. : 329.4K) as a tracer for n-pentane was added to n-pentane. Similarly, as a tracer for n-tridecane, 7.0vol.% tetraline ($C_{10}H_{12}$, b.p. : 480.7K) was added to n-tridecane.

Table 2 summarizes the experimental conditions for the experiments using C5/C13. The injected quantity of all fuels was 10mg, and then the overall air excess ratio was 25 due to the limitation of the maximum cylinder pressure in RCEM. Figure 3 shows the P-T diagram for C5/C13. These P-T diagrams were depicted by the prediction on vapor-liquid equilibrium using SUPERTRAPP [10]. This prediction is based on Peng-Robinson equation of state. The condition of the fuel, which is injected into the combustion chamber,

Table 1 Mixing fraction of each tracer for LIF

X_{C5H12} : Mole fraction of n-pentane
V_{C5H12} : Volume fraction of n-pentane

X_{C5H12}	0.0	0.25	0.5	0.75	1.0
V_{C5H12}	0.0	0.14	0.32	0.59	1.0
Acetone [vol.%]	-	0.6	1.5	2.8	5
Tetraline [vol.%]	7	5.9	4.6	2.7	-

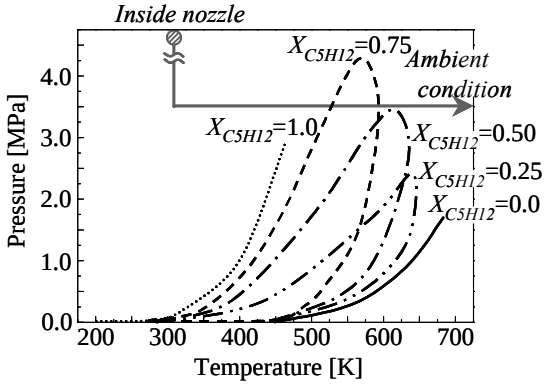

Figure 3 Predicted pressure-temperature diagram for C5/C13

Table 2 Experimental conditions for LIF

RCEM Condition	
Equivalent crank speed	200 r.p.m
Compression ratio	15
Water jacket temperature	353 K
Ambient Condition	
Ambient gas	N_2 : 100 %
Initial cylinder pressure	0.1 MPa
Ambient pressure at TDC	3.4 MPa
Ambient temperature at TDC	750 K
Ambient density at TDC	15 kg/m^3
Ambient viscosity at TDC	32.9 μPa·s
Ambient specific heat at TDC	1117 J/kg·K
Injection Condition	
Orifice diameter	0.20 mm
Injection pressure	15 MPa
Injection velocity	151 m/s
Injection timing	5.0 deg.BTDC
Injection duration	2.0 ms
Injection quantity	10 mg
Excess-air ratio	25
Fuel temperature	353K

is represented in this figure as the bold line. The fuel passes through the two-phase region of these mixed fuels in the case of X_{C5H12}=0.75. Accordingly, it is expected that these mixed fuels will improve atomization and vaporization characteristics owing to the selective flash boiling process. In order to avoid quenching due to oxygen at high pressures encountered, this experiment was conducted without firing by using N_2 gas instead of ambient air.

Figure 4 illustrates an optical system for Mie scattering and LIF. Nd:YAG laser (Spectra-Physics : PIV400) at 266nm was used for excitation light source. In order to form a laser sheet (thickness : 0.5mm), the laser beam was transmitted to two cylindrical lenses and this laser sheet was passed through the spray axis. Fluorescence and scattered light were recorded by ICCD cameras (Hamamatsu : C2925). The camera gain was adjusted so that the peak intensity was less than the saturation limit of the camera. Figure 5 displays the fluorescence spectra of each tracer. Bandpass filters (center wavelength : 407nm, half width : 70nm / center wavelength : 265.7nm, half width : 16.7nm) were placed in front of camera lenses in order to capture fluorescence and scattered light, respectively. However, as can be seen from this figure, fluorescence of tetraline and acetone could not be simultaneously detected due to overlapped fluorescence spectra.

4. Experimental results for spray evaporation

LIF and Mie scattering images are shown in Figure 6. From these images sequences, it can

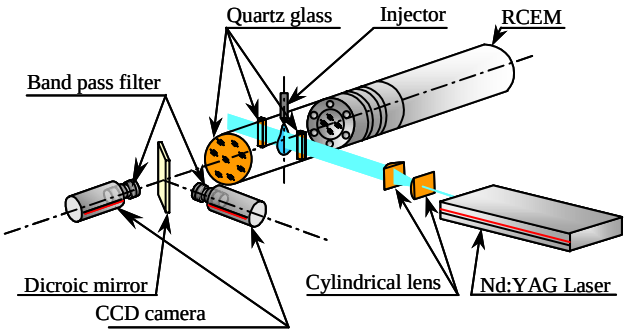

Figure 4 Optical system for Mie scattering and LIF

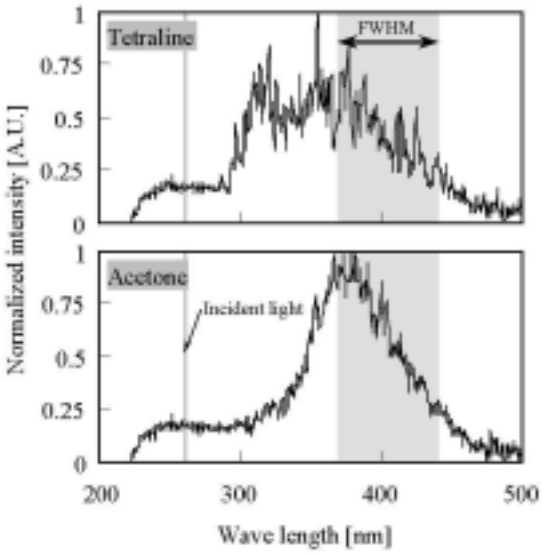

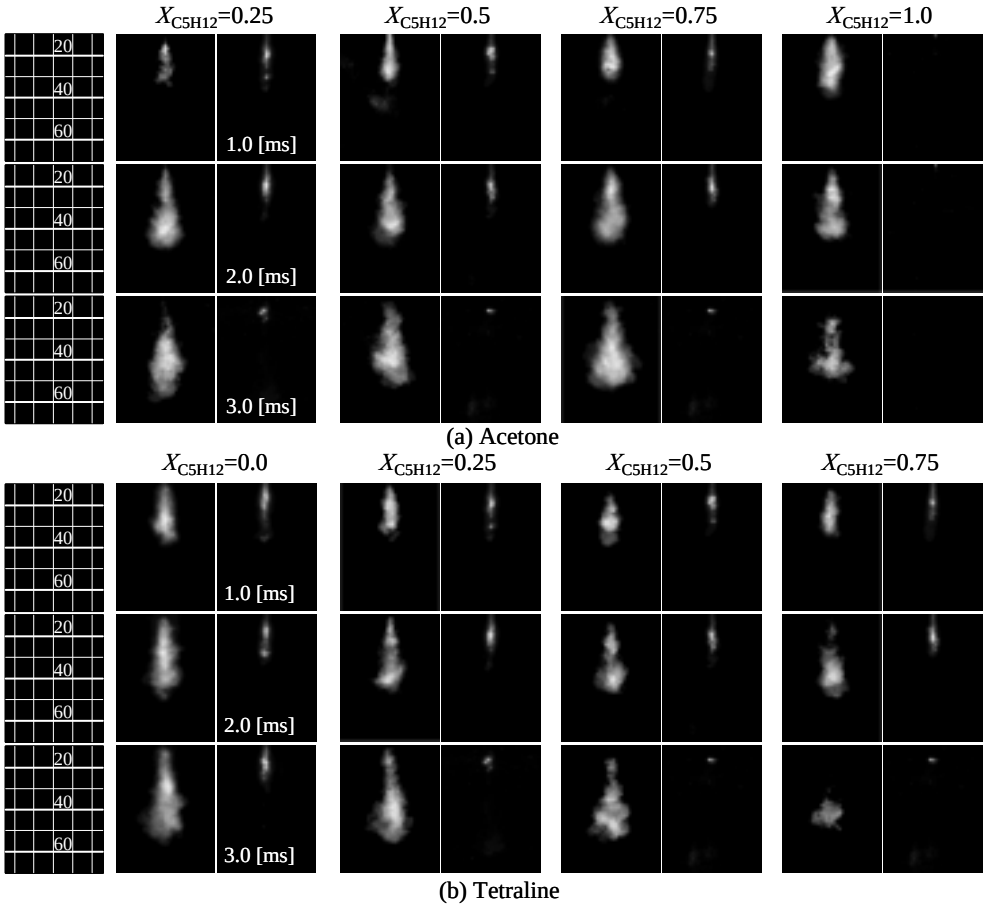

Figure 6 LIF and Mie scattering images (left : LIF , right : Mie scattering)

be seen that liquid-phase penetrations are almost constant for all fuels with the time from injection start, while the weak intensity of the Mie-scattered light at t=3.0ms is owing to end of fuel injection. While vapor-phase penetration is not varied in spite of changing mole fraction, liquid-phase penetration is slightly shortened with increase in the mixing fraction of

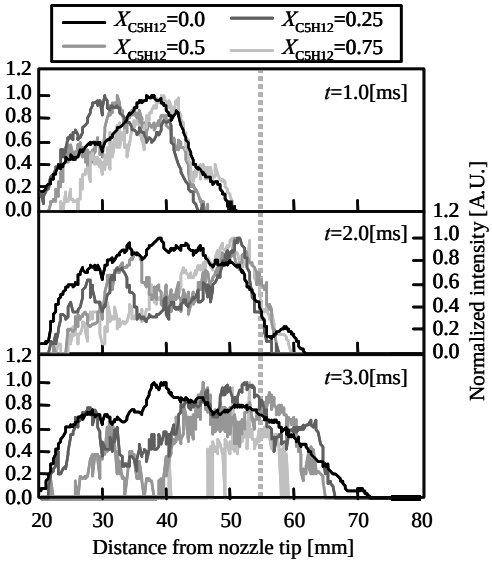

Figure 7 Spatial distributions of LIF intensity for mixed fuels in axial direction

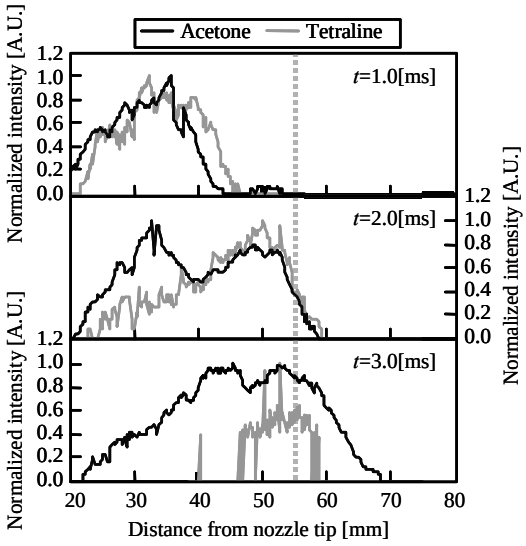

Figure 8 Spatial distributions of LIF intensity in axial direction (X_{C5H12}=0.75)

n-pentane at t=1.0, 2.0ms. It can be estimated that this result is derived from the early stage vaporization of high volatility fuel.

Figure 7 indicates the fluorescence intensity distributions from tetraline in C_{13} fuel in axial direction. The intensity distribution is normalized by maximum intensity of each mixing fraction. The higher intensity region of tetraline moves into the downstream portion of the fuel spray with increasing mole fraction of n-pentane. In particular, fluorescence for X_{C5H12}=0.75 is located only in 45-60mm from nozzle tip.

Figure 8 represents the fluorescence intensity distributions of tetraline and acetone for X_{C5H12}=0.75. Although high concentration region of acetone is located upstream of spray, that of tetraline exists mainly in downstream side of the spray as time passes. The result indicates that the mixture of high volatility fuel broadens near the nozzle tip due to rapid vaporization. Low volatility fuel such as C_{13} fuel moves mainly downstream of the spray, because fuel droplets become lower volatility due to the rapid vaporization of high volatility fuel at droplet surface.

5. Model formulation for multicomponent spray evaporation

Figure 9 shows the flowchart of the model presented here. In this study, this multicomponent fuel evaporation model was incorporated into KIVA3V code. The numerical calculations were carried out for C5/C13 mixed fuel under the same conditions with the experiments.

In original KIVA3V, fuel properties are given at each temperature, and the effect of pressure on the fuel properties is not considered. In addition, liquid density is constant regardless of a change in temperature. Therefore, it is necessary to estimate the accurate fuel properties at each pressure and temperature for the investigation of fuel property effect. In our model, the source code of NIST Mixture Property Database was introduced in KIVA3V, and properties of multicomponent fuel were estimated at given pressure and temperature. NIST Mixture Property Database allows to estimate the properties of the mixture with 20 components. However, NIST Mixture Property Database cannot estimates surface tension and diffusion coefficient of a multicomponent fuel. Therefore, surface tension σ was calculated by the following equation [11].

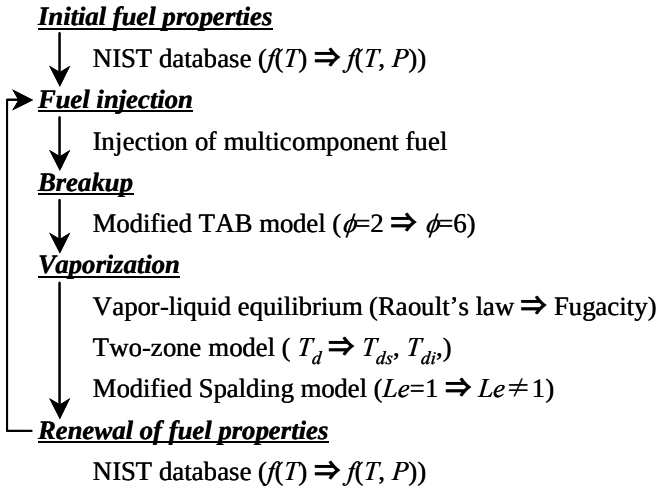

Figure 9 Flowchart of multicomponent fuel spray model

$$\sigma_m^{1/4} = \sum_{i=1}^{n} [P_i](\rho_{Lm} x_i - \rho_{Vm} y_i) \quad (1)$$

n : number of component , $[P_i]$: parachor of component i
ρ_{Lm} : molecular density in liquid phase, ρ_{Vm} : molecular density in vapor phase
x_i : mole fraction of component i in liquid phase
y_i : mole fraction of component i in vapor phase

In addition, diffusion coefficient D_{12} is represented by the following equation [11].

$$D_{12} = \frac{10^{-3} T^{1.75} \left[(M_1 + M_2)/M_1 M_2\right]^{1/2}}{P\left[(V_D)_1^{1/3} + (V_D)_2^{1/3}\right]^2} \quad (2)$$

T : temperature , P : pressure , V_D : diffusion volume
M_1 : molecular weight of component 1
M_2 : molecular weight of component 2

In the case of multicomponent fuel, temperature and mixing fraction in liquid droplet are varied every moment due to the evaporation of each component from droplet surface. Hence, the fuel properties in all parcels were renewed at each time step.

In original KIVA3V, fuel is ideal fluid, and liquid-vapor equilibrium on droplet surface is estimated by Raoult's law. In present model, fuel is regarded as non-ideal fluid, and liquid-vapor equilibrium is estimated using fugacity. Then, the compositions of liquid and vapor phases for each component at droplet surface were determined by the following Peng-Robinson equation of state which takes account for the interaction between each molecule.

$$P = \frac{RT}{V-b} - \frac{a\alpha}{\left(V^2 + 2Vb - b^2\right)} \quad (3)$$

$$\alpha = \left[1 + \left(0.37464 + 1.54226\omega - 0.26992\omega^2\right)\left(1 - T_r^{0.5}\right)\right]^2 \quad (4)$$

$$T_r = T / T_c \quad (5)$$

P : pressure , T : temperature , V : volume
R : gas constant , ω : eccentric coefficient
T_C : critical temperature
a , b : constant

At high ambient pressure, the ambient gases dissolved into the fuel droplet. This process has an important effect on fuel properties, especially surface tension. Hence, the quantity of dissolved ambient gas, and transport properties were calculated for liquid droplet containing ambient gas using this liquid-vapor equilibrium estimation. Two-zone model [12], in which fuel droplet is divided into droplet surface and interior, was employed in order to calculate droplet temperature. In two-zone model, temperature distribution in fuel droplet can be simply expressed, because heat energy is transferred from droplet surface to droplet interior. In addition, two-zone model prevents fuel droplet from over-vaporizing, since only droplet surface is evaporated at critical temperature.

In original KIVA3V, original Spalding model is employed as droplet vaporization model, and this model supposes that mass and heat transfer term are equivalent (Lewis number Le=1.0). An important modification to the Spalding model was proposed by Abramzon and Sirignano [13]. The following improved Spalding model individually calculates both of mass transfer and heat transfer terms ($Le \neq 1.0$).

$$\dot{m} = 2\pi \cdot r_{ds} \cdot (\rho \cdot D)_s \cdot Sh \cdot B_M \cdot (1 + B_M)^{-0.7}$$

$$\dot{Q}_{g-d} = 2\pi \cdot r_{ds} \cdot k_{ds} \cdot Nu \cdot (T_{g\infty} - T_{ds}) \cdot (1 + B_T)^{-0.7} \quad (7)$$

$$B_M = \frac{Y_{ds} - Y_\infty}{1 - Y_{ds}} \quad (8)$$

$$B_T = \frac{c_{ps} \cdot (T_{g\infty} - T_{ds})}{Q_{vap}} \quad (9)$$

$\dot{m}$: evaporation rate , r_{ds} : radius at droplet surface
ρ_s : density on droplet surface , D_s : diffusion coefficient
Sh : Sherwood number , B_M : term of mass transfer
$\dot{Q}_{g-d}$: quantity of heat transfer
k_{ds} : thermal diffusivity on droplet surface
Nu : Nusselt number , $T_{g\infty}$: ambient temperature
T_{ds} : temperature at droplet surface
B_T : term of heat transfer
Y_{ds} : mass fraction on droplet surface
Y_∞ : mass fraction at infinity
c_{ps} : specific heat on droplet surface
Q_{vap} : evaporation enthalpy per unit mass

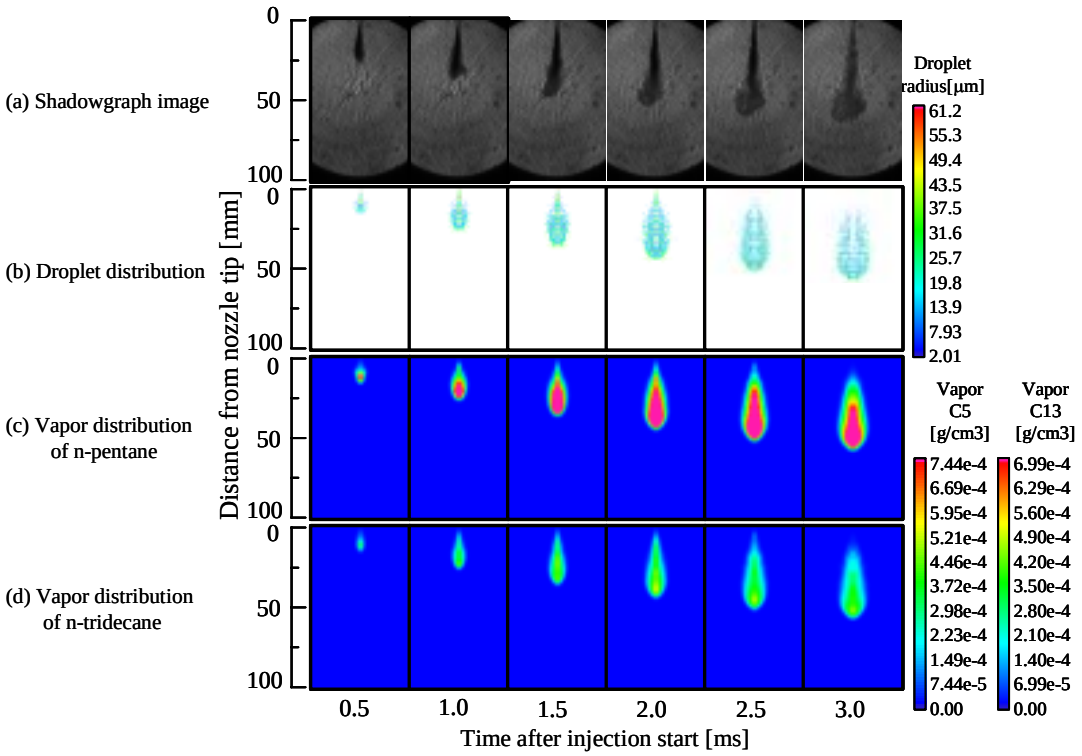

6. Numerical results for spray evaporation

Figure 10 shows the droplet distribution and vapor distributions for n-pentane and n-tridecane in C5/C13 mixed fuel at X_{C5H12}=0.75. According to the calculations for mixed fuels of X_{C5H12}=0.0 - 1.0, high vapor concentration region of n-pentane is located from upstream to downstream of the spray in spite of a change in mixing fraction. On the other hand, high vapor concentration region of n-tridecane is mainly located in downstream of fuel spray. The numerical results of multicomponent fuel spray vaporization are consistent well with the experimental results shown in Figure 6.

Figure 11 indicates the temporal change in vapor mass of n-pentane and n-tridecane. Vapor mass of n-pentane increases with an increase in the mole fraction of n-pentane. On the other hand, vapor mass of n-tridecane linearly increases with an increase in the mixing

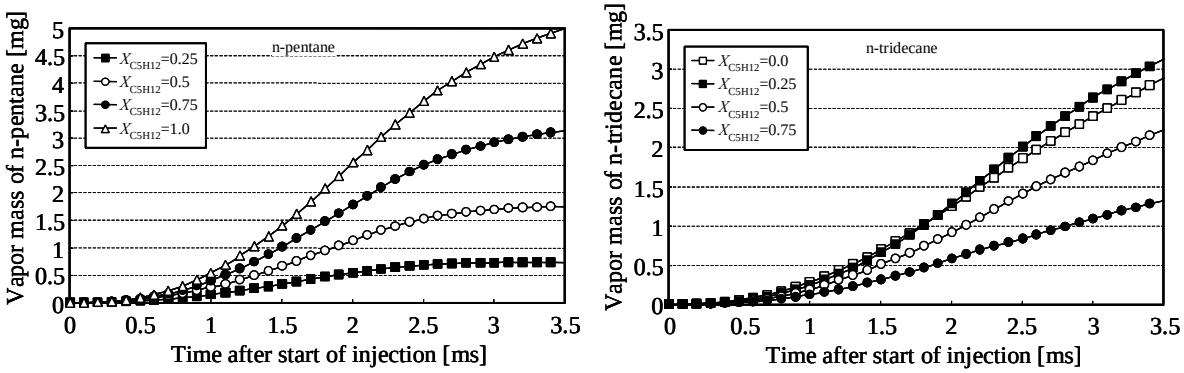

Figure 11 Temporal change in vapor mass of C5 and C13

fraction of n-tridecane at early stage of fuel injection. However, vapor mass of n-tridecane for X_{C5H12}=0.25 is more than that for pure n-tridecane (X_{C5H12}=0.0) after t_{inj}=2.0ms. As can be seen from Figure 3, the saturated vapor line of low volatility fuel (n-tridecane) is shifted to high pressure and low temperature side. In other words, n-tridecane becomes high volatility. Thus, the lower volatile fuel of n-tridecane is effectively vaporized by mixing n-pentane component through the two-phase region effect.

7. Conclusion

The following conclusions are obtained from this study.

1. Vapor-phase penetration is not varied with the variation of fuel composition. But liquid-phase penetration is slightly shortened with increasing mixing fraction of high volatile fuel.
2. Low boiling point component included in mixed fuel mainly evaporates in upstream portion of spray and high boiling point fuel vapor distributes near downstream region.
3. Multicomponent fuel evaporation model was proposed considering vapor-liquid equibilium. Furthermore, detailed fuel properties at each pressure and temperature are calculated in this model.
4. Spatial distribution of the vapors in muticomponent fuel spray can be estimated quantitatively with this proposed model. The calculated spray structure including the vapor distribution has a good agreement with the actual multicomponent fuel spray field.

References

[1] Jin J D and Borman G L 1985 SAE Paper 850264
[2] Chen G, Aggarwal S K, Jackson T A and Switzer G L 1997 Atomization and Spray 7 317-337
[3] Ayoub N S and Reitz R D 1995 SAE Paper 950285
[4] Ayoub N S and Reitz R D 1995 SAE Paper 952425
[5] Lippert A M and Reitz R D 1997 SAE Paper 972882
[6] Abraham J and Magi V 1998 SAE Paper 980511
[7] Nagaoka M, Ohsawa K, Crary B, Yamada T, Sugiura S and Imatake N 1997 SAE Paper 970878
[8] Senda J, Higaki T, Sagane Y, Fujimoto H, Takagi Y and Adachi M 2000 SAE Paper 2000-01-0280
[9] Senda J and Fujimoto H 2001 SAE Paper 2001-01-1071
[10] Ely J F and Huber M L 1992 *NIST Thermophysical Properties of Hydrocarbon Mixtures Database (SUPERTRAPP) Version 1.0 User's Guide*
[11] Ooe S 1985 *Estimation of constant number in physical-properties (in Japanese)* published by Nikkankougyou-shinbun
[12] Curtis E W, Uludogan A and Reitz R D 1995 SAE Paper 952431
[13] Abramzon B and Sirignano W A 1989 Int. J. Heat Mass Transfer 32(9) 1605-1618